International Journal of Automotive Technology, Vol. 12, No. 2, pp. 207–212 (2011)
DOI 10.1007/s12239–011–0025–9

1229–9138/2011/057–07

SENSORLESS ADAPTIVE SPEED CONTROL OF A PERMANENT-MAGNET DC MOTOR FOR ANTI-LOCK BRAKE SYSTEMS

S. B. CHOI*

Mechanical Engineering Department, KAIST, Daejeon 305-301, Korea

(Received 11 December 2009; Revised 30 August 2010)

ABSTRACT–An adaptive control algorithm was developed for the sensorless speed control of a permanent-magnet DC motor directly connected to the hydraulic pump of an antilock brake system. Due to the severe cost and reliability constraints of the application, the motor speed was controlled by a very simple on-off switching method, in which the only measurement required is the voltage across the control switch. The motor speed was calculated solely from the back-EMF voltage during the period of the control cycle when the switching controller is in the switch-off mode. The stability of the developed adaptive-switching control algorithm was proven mathematically and confirmed experimentally in several vehicle tests over a wide range of target speeds and pump-load conditions. The accuracy and the response time of the controller can easily be tuned by adjusting a single tuning parameter. The switching frequency of the controller can also easily be tuned by adjusting the over- and undershoot thresholds independently from the accuracy of the speed-tracking control.

KEY WORDS : ABS, DC motor, Speed control, Sensorless

NOMENCLATURE

i : current
k : discrete time steps, $k = 1, 2, 3, \ldots$
k_o : back-EMF voltage gain
k_1 : motor dynamic gain, inverse of the motor time constant
k_g : adaptive control gain
k_t : motor torque gain
R : resistance
t^k : time during the kth control time period when the motor power is switched off
T_L : motor external torque load
T_M : motor drive torque
V^k : a positive scalar function, $k = 1, 2, 3, \ldots$
V_s : supply voltage
$\Delta\omega_1$: motor power-on undershoot threshold, a positive constant
$\Delta\omega_2$: motor power-off overshoot threshold, a positive constant
ω : actual motor speed
ω_f : final steady-state motor speed when the motor is powered for a long time
ω_{target} : target motor speed
ω^k : motor speed when the motor power is switched off during the kth control time period
$\hat{\omega}$: estimated motor speed
$\hat{\omega}_f^k$: steady-state (final) motor speed estimated during the kth control time period

*Corresponding author. e-mail: sbchoi@kaist.ac.kr

1. INTRODUCTION

Electric motors and controllers have been in use for a long time in a very wide spectrum of applications. At the one end of the spectrum are expensive, high-precision controllers; at the other end are the low-cost but very reliable controllers in used in applications such as automotive subsystem controls. There have been many efforts to reduce the cost and improve the reliability of these systems by controlling motor position or speed without a sensor (Leephakpreeda, 2002; Jung and Ha, 2000; Su and McKeever, 2004; Hernandez and Sira-Ramirez, 2001; Dzung and Phuong, 2005; Lee *et al*., 2005; Kim and Youn, 2002). From the control point of view, many advanced techniques have been developed to deal with the nonlinearities and uncertainties including unknown external disturbances (Baruch *et al*., 2001; Kang and Kim, 2001; Machbub *et al*., 2001; Nam, 2001).

Figure 1 describes the flow path of brake fluid in the hydraulic circuit of an antilock brake system (ABS). The supply pressure of the brake system is provided by the driver depressing the brake pedal. The brake fluid supplied to the wheel is dumped to the low-pressure accumulator and pumped back to the master cylinder. The accumulator has sufficient capacity to hold all the dumped fluid. If the pump fails or does not run fast enough, then the driver cannot generate sufficient brake pressure even if the pedal

is fully depressed. If the pump runs too fast, it will not hurt the braking performance but can cause severe noise.

To address the issue of noise during ABS activation, it is recommended to keep the pump speed as low as possible or to limit the maximum speed by precise speed-tracking control. Due to the severe cost and the reliability constrains in this system, a control system was designed for an ABS pump with a permanent-magnet DC motor with the following characteristics:

- The motor speed is controlled by on-and-off–mode control
- The motor speed is measured indirectly only when the control is in the off mode
- The load of the pump changes very rapidly but cannot be measured or estimated

The speed of DC motors can be measured indirectly using back-EMF voltage, current and motor parameters (Zaharin and Taib, 2003). In this study of the ABS motor and control-circuit system, only the voltage across the control switch was measured due to the above constraints, which are typical of motor-speed control for conventional production ABS. When the switch is on, the measured voltage is equal to the battery supply voltage. When the switch is off, the current across the switch is zero, and the measured voltage is proportional to the motor speed. These characteristics make speed control very difficult. The conventional ABS controller exploits a rule-based control algorithm for motor-speed control. The motor power switch-on time is determined heuristically as a function of the speed error at the moment of switch-off and given as a look-up table. Therefore, it requires a long time to tune the table contents; satisfying the error-tracking requirement and the switching-frequency constraint is not an easy task. Furthermore, the error convergence and control stability cannot be proven. The goal of the proposed control design was to minimize the deviation of the motor speed from the target speed without using a time-consuming heuristic, rule-based algorithm. To achieve this goal, an adaptive speed-estimation method was developed by considering the fact that variation of external load on the motor has a significant effect on the control performance but is totally unpredictable. The stability of the estimation method was proven mathematically, and the performance of the controller was experimentally evaluated in a test vehicle.

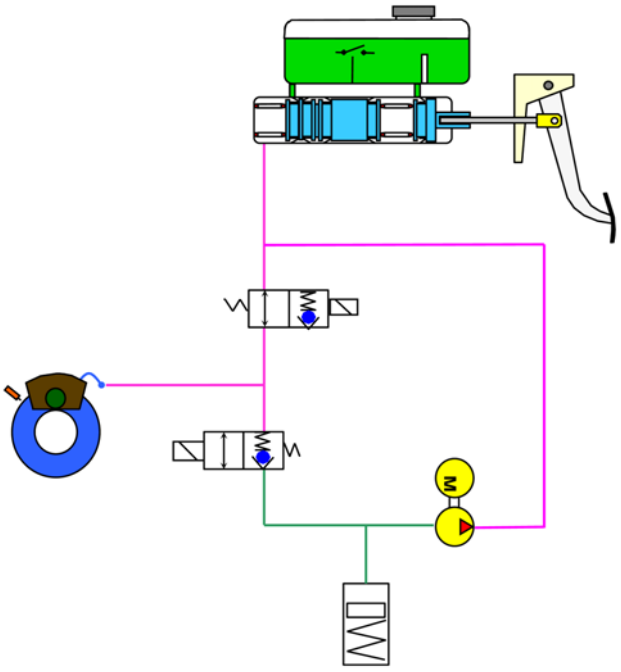

Figure 1. Diagram of brake-fluid flow in ABS hydraulic circuit.

2. PUMP/MOTOR MODEL

For a simple DC motor circuit, the voltage and the current are related to the motor speed as follows:

$$V_s = iR + k_0\omega \tag{1}$$

where V_s is the supply voltage to the circuit, R the resistance, k_0 a constant, and ω the motor speed. Because the output torque T_M of the motor is proportional to the current, the torque is described as follows:

$$T_M = k_i i \tag{2}$$

From the force-balance condition, the motor speed is described as follows:

$$J\dot{\omega} = T_M - T_L \tag{3}$$

where J is the angular moment of inertia of the motor and the pump and T_L the external pumping load on the motor. Combining Equations (1), (2) and (3) yields:

$$\dot{\omega} = -\frac{k_i k_0}{J\,R}\left(\omega - \frac{k_i V_s - J\,R T_L}{k_i k_0}\right) \tag{4}$$

As k_i, k_o, J and R are known constants, and the motor speed converges to $(k_iV_s\text{-}JRT_L)/(k_ik_0)$ at the steady state, the dynamics of the system during the power-on mode can be modeled as a simple first-order system as follows:

$$\dot{\omega} = -k_1(\omega - \omega_f) \tag{5}$$

where k_1 has the physical meaning of the inverse of the motor time constant and ω_f is the final speed of the motor when it is powered for a sufficient time to reach the steady state. Due to the characteristics of the DC motor, the motor speed is saturated, and the final speed decreases in proportion to the external load on the motor. In this case, the external torque load is proportional to the master-cylinder pressure (pressure head), which is unknown. To make

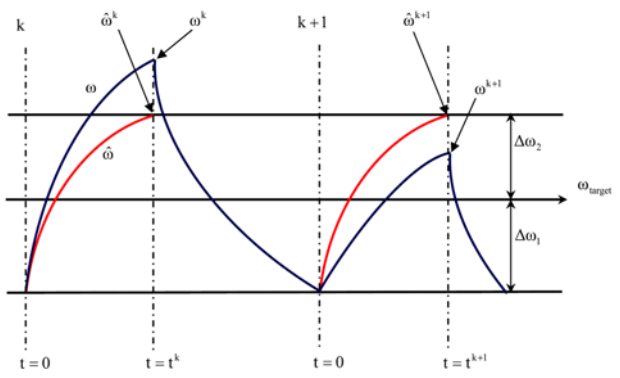

Figure 2. Switching-mode control concept and definitions.

matters worse, the load can drop rapidly if the low-pressure accumulator (LPA) is empty.

3. CONTROL ALGORITHM

For the on-off-mode motor-speed control algorithm, two mode-switching thresholds are defined around the target speed ω_{target}. When the switch is off, the motor speed can be calculated directly from the measured back-EMF voltage. When the switch is on, the motor speed is estimated using the first-order system model described in Equation (5) and the estimated final motor speed. Motivated by the pump/motor model described in Equation (5), a motor-speed-estimation algorithm was proposed as follows:

$$\dot{\hat{\omega}} = -k_1(\hat{\omega} - \omega_f^k) \tag{6}$$

where $\hat{\omega}$ is the estimated motor speed and ω_f^k the estimated steady-state motor speed during the kth period of the switching control step described in Figure 2. It should be noted that k_1 is the only modeling parameter that must be identified. The time period is defined as that from the beginning of the power-on mode to the end of the power-off mode, which is also the beginning point of the next power-on mode. The motor is switched on if the measured actual speed (ω) falls below a certain threshold with respect to the target speed and switched off if the estimated speed exceeds a certain threshold with respect to the target speed, e.g.:

$$\begin{aligned} &if\ \ \omega < \omega_{target} - \Delta\omega_1 \Rightarrow ON \\ &if\ \ \hat{\omega} > \omega_{target} - \Delta\omega_2 \Rightarrow OFF \end{aligned} \tag{7}$$

If the estimation of the motor-speed dynamics given in Equation (6) is accurate, i.e., the estimated steady-state motor speed is same as the true steady-state speed, then the motor speed measured immediately after the control is switched to the off mode (ω^k) should be equal to $\omega_{target} + \Delta\omega_2$. The accuracy of the developed model described in Equation (5) is affected by several modeling parameters. For example, the motor resistance R is not necessarily a constant; rather, it is a function of operating temperature. However, the main cause of the speed error ($\omega^k - \omega_{target} - \Delta\omega_2$) lies in the uncertainty of the motor-torque load, which has a direct effect on the steady-state motor speed (ω_f); therefore, a final speed-adaptation algorithm as a function of the speed error was suggested as follows:

$$\omega_f^k = \omega_f^{k-1} + k_g(\omega^{k-1} - \omega_{target} - \Delta\omega_2) \tag{8}$$

where ω^{k-1} is the measured motor speed at the point where the motor power is switched off during the k-1st control time period. The adaptation gain k_g is the only parameter that must be tuned to meet the control requirements. As the gain k_g is increased, the motor-load model is updated more rapidly and the period of overshoot or undershoot of the motor speed from the target speed is minimized. However, excessive gain can make the control scheme unstable.

4. STABILITY ANALYSIS OF ADAPTIVE CONTROL ALGORITHM

For the purposes of the stability analysis, it is assumed that the switching thresholds $\Delta\omega_1$ and $\Delta\omega_2$ are constants. To simplify the analysis, it is further assumed that the target motor speed ω_{target} is constant from time period *k-1* to *k*. Because the adaptive control is a continuous process, a few large jumps or the continuous but slow change of the target speed will cause no differences in the results of the analysis.

Defining the time at the beginning of the k^{th} period as t = 0, the motor dynamics given in Equation (5) can be integrated as follows:

$$\omega(t) = -(\omega_f - \omega_{target} + \Delta\omega_1)e^{-k_1 t} + \omega_f \tag{9}$$

In the same manner, the estimated motor speed described in Equation (6) can be integrated during the same time period as follows:

$$\hat{\omega}(t) = -(\omega_f^k - \omega_{target} + \Delta\omega_1)e^{-k_1 t} + \omega_f^k \tag{10}$$

The moment of switching to the off mode is determined by the following condition:

$$\hat{\omega}(t^k) = \omega_{target} + \Delta\omega_2 \tag{11}$$

Therefore, from Equations (10) and (11):

$$e^{-k_1 t} = \frac{\omega_f^k - \omega_{target} - \Delta\omega_2}{\omega_f^k - \omega_{target} + \Delta\omega_1} \tag{12}$$

From Equations (9), (10) and (12):

$$\omega^k - \hat{\omega}^k \equiv \omega(t^k) - \hat{\omega}(t^k)$$

$$= -(\omega_f - \omega_f^k)e^{-k_1 t} + \omega_f - \omega_f^k$$

$$= (\omega_f - \omega_f^k)\frac{\Delta\omega_1 + \Delta\omega_2}{\omega_f^k - \omega_{target} + \Delta\omega_1} \quad (13)$$

Equation (8) can be rewritten as:

$$\omega_f - \omega_f^k = \omega_f - \omega_f^{k-1} - k_g(\omega^{k-1} - \omega_{target} - \Delta\omega_2)$$

$$= \omega_f - \omega_f^{k-1} - k_g(\omega^{k-1} - \hat{\omega}^{k-1}) \quad (14)$$

Motivated by Equation (13), a positive scalar function is defined during the period k as follows:

$$V^k = \frac{1}{2}\left(\frac{\omega_f^k - \omega_{target} + \Delta\omega_1}{\Delta\omega_1 + \Delta\omega_2}\right)^2 (\omega^k - \hat{\omega}^k)^2 + \frac{1}{2}(\omega_f - \omega_f^k)^2 \quad (15)$$

Combining Equations (13), (14) and (15):

$$V^k = (\omega_f - \omega_f^k)^2$$

$$= [(\omega_f - \omega_f^{k-1}) - k_g(\omega^{k-1} - \hat{\omega}^{k-1})]^2$$

$$= (\omega_f - \omega_f^{k-1})^2 - 2k_g(\omega_f - \omega_f^{k-1})(\omega^{k-1} - \hat{\omega}^{k-1}) + k_g^2(\omega^{k-1} - \hat{\omega}^{k-1})^2$$

$$= (\omega_f - \omega_f^{k-1})^2 - 2k_g(\omega_f - \omega_f^{k-1})^2\frac{\omega_f^{k-1} - \omega_{target} + \Delta\omega_1}{\Delta\omega_1 + \Delta\omega_2} + k_g^2(\omega^{k-1} - \omega^{k-1})^2$$

$$= V^{k-1} - k_g\left(2\frac{\omega_f^{k-1} - \omega_{target} + \Delta\omega_1}{\Delta\omega_1 + \Delta\omega_2} - k_g\right)(\omega^{k-1} - \hat{\omega}^{k-1})^2 \quad (16)$$

Because the switch-off threshold ($\omega_{target} + \Delta\omega_2$) is always set to be lower than the final steady-state motor speed (ω_f):

$$\omega_f^{k-1} - \omega_{target} + \Delta\omega_1 \geq (\omega_{target} + \Delta\omega_2) - \omega_{target} + \Delta\omega_1 = \Delta\omega_1 + \Delta\omega_2 \quad (17)$$

Using the inequality condition (17), Equation (16) can be rewritten as:

$$V^k \leq V^{k-1} - k_g(2 - k_g)(\omega^{k-1} - \hat{\omega}^{k-1})^2 \quad (18)$$

Therefore, it is guaranteed that $V^k < V^{k-1}$, i.e., the adaptive controller is stable for any k_g less than 2, and the velocity-estimation error $\omega^k - \hat{\omega}^k$ converges to zero. Also, Equation (13) shows that if $\omega^k - \hat{\omega}^k$ converges to zero, $\omega_f - \omega_f^k$ also converges to zero. Therefore, this proves that the adaptive-switching control algorithm described in Equations (7) and (8) is asymptotically stable.

5. DESIGN EXAMPLE AND EXPERIMENTAL RESULTS

Figure 3 shows an example of the motor controller implemented in the ABS of a Ford Windstar minivan using the Simulink commercial graphic language and control-design tool. The motor dynamic gain (k_1) was here measured to be 30. Theoretically, the motor-speed observer gain (k_g) can be set to any positive value less than 2.0. However, considering the effect of other uncertainties, it is safer to set the gain lower than the threshold. Therefore, the gain was experimentally determined to be 0.5 to guarantee fast adaptation and stability at the same time. Finally, as a trade-off between speed-tracking performance and control-circuit switching frequency, the overshoot threshold ($\Delta\omega_2$) was set to 300, and the undershoot threshold ($\Delta\omega_1$) to 200. Therefore, the peak-to-peak swing of the motor speed was intended to be in the range of –200 to +300 *rpm* around the target speed. The magnitude of the speed swing can be set to be much less. However, it is currently limited by the switching frequency of the motor driver circuit: a reduced swing indicates high-frequency switching, and the switching circuit can be overheated.

Figures 4 and 5 show the results of the motor-speed control during braking with the ABS activated. The target motor speed was set by the ABS algorithm as a function of the dump-valve commands and the estimated vehicle acceleration. As the motor speed can be calculated only when the motor power is switched off, the measured motor speed was not updated during the power-on mode. During

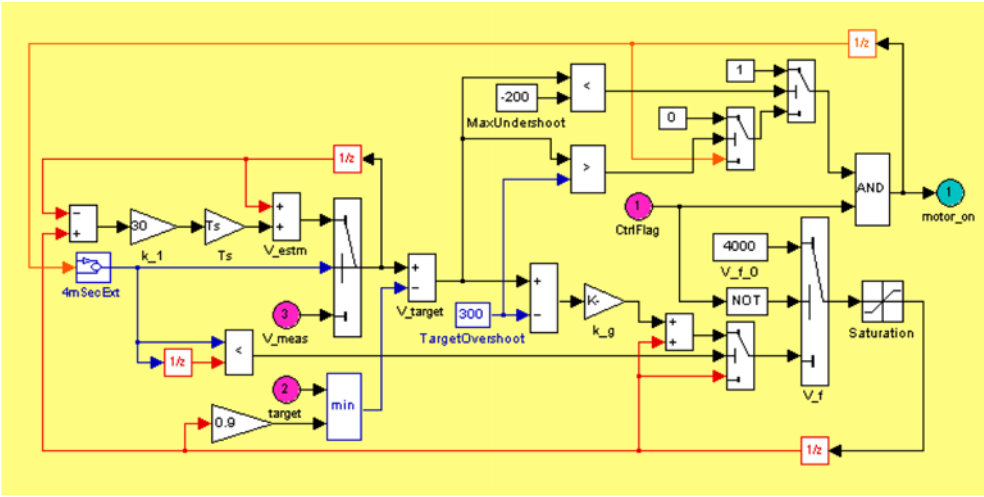

Figure 3. Control algorithm implemented in Simulink.

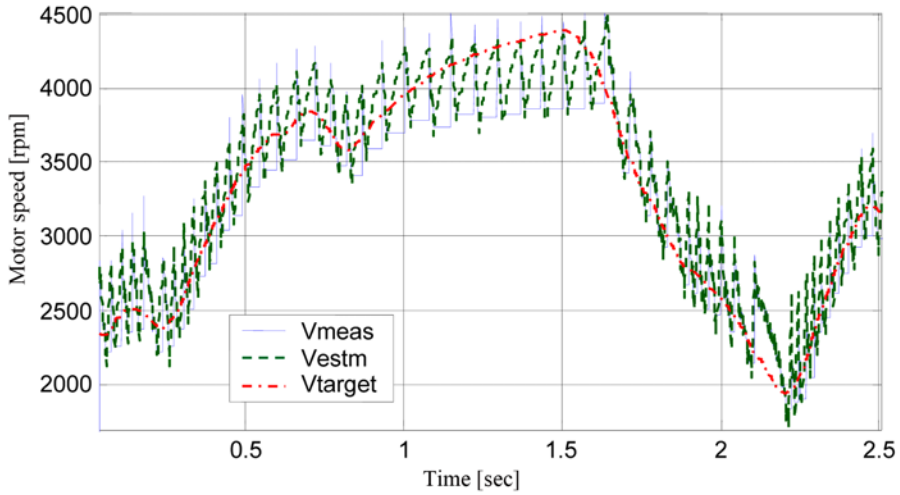

Figure 4. Motor-speed control during ABS activation on a high-Mu road surface.

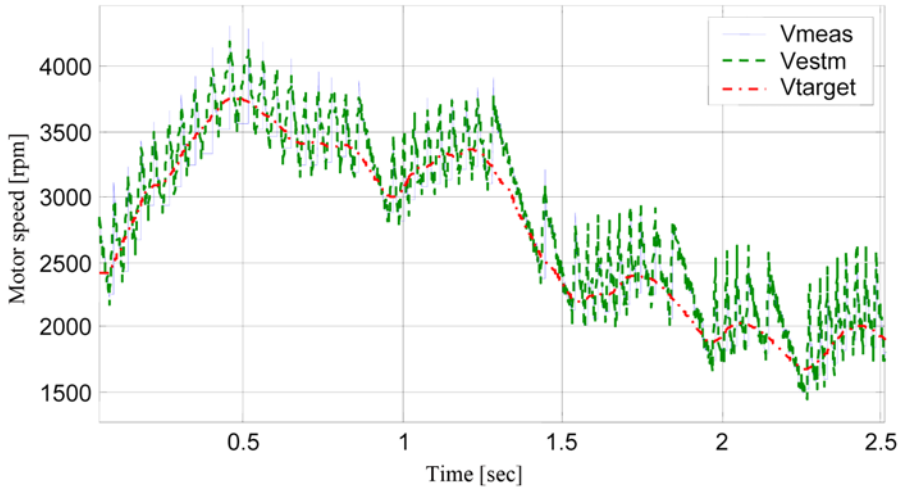

Figure 5. Motor-speed control during ABS activation on a gravel road surface.

the power-on mode, the estimated motor speed was updated using Equation (6). Generally speaking, the motor speed followed the target speed well within the envelope of the thresholds. The varying target speed and the varying power-switching frequency show that the external torque load on the motor was not a constant.

6. CONCLUSIONS

A simple and robust adaptive motor-speed control algorithm was designed and implemented in a conventional, low-cost ABS pump/motor system. The adaptive control algorithm requires only one plant-model parameter and has only one gain requiring tuning. The stability of the control algorithm was proven mathematically, and its robustness was confirmed experimentally in several vehicle tests over a wide range of target speeds and pump-load conditions. The accuracy and the response time of the controller can easily be tuned simply by adjusting the adaptation gain. The speed-swing band of the tracking control and, therefore, the switching frequency of the controller, can be easily and independently tuned by adjusting the over- and the undershoot thresholds.

REFERENCE

Baruch, I. S., Garrido, R., Flores, J. M. and Martinez, J. C. (2001). An adaptive neural control of a DC motor. *Proc. IEEE Int. Symp. Intelligent Control*, 121–126.

Dzung, P. Q. and Phuong, L. M. (2005). Control system DC motor with speed estimator by neural networks. *Proc. Int. Conf. Power Electronics and Drivers Systems*, 1030–1035.

Hernandez, V. M. and Sira-Ramirez, H. (2001). Position control of an inertia-spring DC-motor system without mechanical sensors: experimental results. *Proc. 40th IEEE Conf. Decision and Control*, **2**, 1386–1391.

Jung, D. H. and Ha, I. J. (2000). Low-cost sensorless control of brushless DC motors using a frequency-independent phase shifter. *IEEE Trans. Power Electronics* **15**, **4**, 744–752.

Kang, Y. H. and Kim, L. K. (2001). Design of neuro-fuzzy controller for the speed control of a DC servo motor. *Proc. 5th Int. Conf. Electrical Machines and Systems*, **2**, 731–734.

Kim, K. H. and Youn, M. J. (2002). DSP-based high-speed sensorless control for a brushless DC motor using a DC link voltage control. *Electric Power Components and Systems* **30**, **9**, 889–906.

Lee, S. J., Yoon, Y. H. and Won, C. Y. (2005). Precise speed control of the PM brushless DC motor for sensorless drives. *Proc. 8th Int. Conf. Electrical Machines and Systems*, **1**, 290–295.

Leephakpreeda, T. (2002). Sensorless DC motor drive via optimal observer-based servo control. *Optimal Control Applications & Method* **23**, **5**, 289–301.

Machbub, C., Prihatmanto, A. S. and Cahaya, Y. D. (2001). Design and implementation of adaptive neural networks algorithm for DC motor speed control system using simple microcontroller. *Proc. 4th IEEE Int. Conf. Power Electronics and Drive Systems*, **2**, 479–483.

Nam, S. K. (2001). Fuzzy time delay control for DC servo motor. *Proc. 10th IEEE Int. Conf. Fuzzy Systems*, **1**, 485–488.

Su, G. J. and McKeever, J. W. (2004). Low-cost sensorless control of brushless DC motors with improved speed range. *IEEE Trans. Power Electronics* **19**, **2**, 296–302.

Zaharin, A. and Taib, M. N. (2003). A study on the DC motor speed control by using back-EMF voltage. *Proc. AsiaSENSE Conf.*, 359–364.